Chemical Engineering Journal 315 (2017) 58–66

Contents lists available at ScienceDirect

Chemical Engineering Journal

journal homepage: www.elsevier.com/locate/cej

Concomitant Cr(VI) reduction and Cr(III) precipitation with nitrate in a methane/oxygen-based membrane biofilm reactor

Min Long [a], Chen Zhou [b], Siqing Xia [a,*], Awoke Guadiea [a,c]

[a] State Key Laboratory of Pollution Control and Resource Reuse, College of Environmental Science and Engineering, Tongji University, Shanghai 200092, China
[b] Biodesign Swette Center for Environmental Biotechnology, Arizona State University, USA
[c] Department of Biology, College of Natural Sciences, Arba Minch University, P.O. Box 21, Arba Minch, Ethiopia

HIGHLIGHTS

- Aerobic CH_4 oxidation coupled with denitrification and Cr(VI) reduction are investigated.
- Direct removal of Cr(VI) from ground and drinking water without the addition of precipitant.
- Optimal conditions for concomitant Cr(VI) reduction and Cr(III) precipitation in the methane/oxygen-based MBfR.
- Functional bacteria existed in the methane/oxygen-based MBfR.

GRAPHICAL ABSTRACT

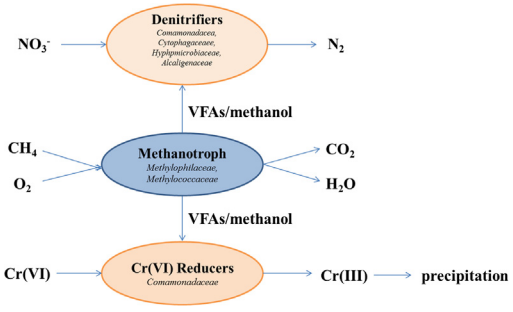

ARTICLE INFO

Article history:
Received 19 November 2016
Received in revised form 5 January 2017
Accepted 6 January 2017
Available online 7 January 2017

Keywords:
Chromium (Cr)
Biofilm
Membrane biofilm reactor (MBfR)
Methane
Nitrate (NO_3^-)

ABSTRACT

A continuously stirred methane (CH_4) and oxygen (O_2)-based membrane biofilm reactor (MBfR) was investigated for removing chromium (Cr) from nitrate (NO_3^-)-contaminated drinking water. Cr(VI) at an initial concentration of 100 μg/L was rapidly reduced to Cr(III) with a removal rate of 89% and a hydraulic retention time of 48 h under normal denitrifying conditions in a methane/oxygen-based MBfR. A microbial community analysis indicated that *Comamonadaceae, Cytophagaceae, Hyphomicrobiaceae* and *Alcaligenaceae* were effective denitrifiers, *Methylophilaceae and Methylococcaceae* were functional methanotrophic bacteria, and *Comamonadaceae* was a kind of Cr(VI) reducers in the reactor. Cr(VI) was reduced to Cr(III), which precipitated and adsorbed onto the biofilm as $Cr(OH)_3$, due to the alkaline produced during denitrification. When the CH_4 pressure increased from 0.02 to 0.03 MPa, the Cr(VI) reduction increased by 40.3%, and the NO_3^- reduction increased by 30.2%. Although the effluent Cr(VI) concentration increased with increasing influent loading, the removal efficiency of Cr(VI) reached the highest level of 99.8% under a high daily loading of 5.76 mg/d. Unlike a H_2-based MBfR, it is possible to remove Cr from water without post-processing, such as precipitation, in a CH_4/O_2-based MBfR.

1. Introduction

Chromium is one of the most widely used metals in industries such as wood preservation, leather tanning, metal finishing, and pigments [1]. These processes result in the discharge of high concentration Cr(VI) into bodies of water and threaten the environment and human health. Chromium (Cr) exists mainly in

* Corresponding author at: No. 1239 Siping Road, Tongji University, Shanghai 200092, China.
E-mail address: siqingxia@tongji.edu.cn (S. Xia).

http://dx.doi.org/10.1016/j.cej.2017.01.018
1385-8947/

trivalent [Cr(III)] and hexavalent [Cr(VI)] forms. While trivalent chromium has low toxicity and can easily removed from water via precipitation [2], Cr(VI) is a strong oxidant that is toxic, mutagenic, teratogenic, and carcinogenic [3]. The use and release of Cr are strictly regulated in many countries. For example, the U.S. Environmental Protection Agency has set the maximum contaminant level (MCL) for Cr in drinking water at 100 μg/L [4].

Nitrate is a common oxidized contaminant in drinking water and groundwater [5]. Removing nitrate (NO_3^-) and nitrite (NO_2^-) from water is becoming increasingly important due to adverse health impacts on humans. For example, NO_3^- in drinking water is suspected to be a possible cause of methaemoglobinaemia in infants [6]. Biological denitrification has been widely carried out for the treatment of such water sources (containing high nitrate) to reduce NO_3^- to NO_2^-, nitric oxide (NO), nitrous oxide (N_2O), and finally to nitrogen gas (N_2) [5].

Biodegradation of Cr(VI) under denitrification condition has been proposed and studied in the past few years to create the synergistic degradation of two contaminants at the same time. The influent Cr(VI) concentration higher than 1.0 mg Cr/L exerted a clear inhibitory effect on sulfur-based autotrophic denitrification [7]. However, influent Cr(VI) below 10 mg Cr/L exerted no significantly inhibitory effect on Cr(VI) reduction by heterotrophic denitrifiers and Cr(VI) reducing bacteria, while an increase from 10 to 20 mg Cr/L led to Cr(VI) accumulation in the effluent [7]. Cr(VI) at low levels stimulate microbial growth [8], but the high concentrations of Cr(VI) can inhibit microbial growth by altering enzyme conformation and blocking essential functional groups, and affect their denitrifying capacity [9].

Methane (CH_4) oxidation coupled with denitrification occurs under both anoxic and aerobic conditions. The anoxic process is accomplished by slow-growing microorganisms. By contrast, aerobic methane oxidation coupled with denitrification (AME-D) appears to be feasible, because the aerobic methanotrophs can be enriched from various environmental samples and are able to grow rapidly [10]. In the AME-D process, aerobic methanotrophs are capable of oxidizing CH_4 and releasing soluble organic compounds for the coexisting denitrifiers as carbon sources [11]. Oxygen plays a complex role in the microbial community, as one of its functions is to inhibit denitrification [12], and it is also essential for CH_4 oxidation [13]. Therefore, dissolved oxygen (DO) is a key factor that should be controlled properly.

Membrane biofilm reactors (MBfRs) are novel technology that has been used to remove inorganic anions such as nitrate (NO_3^-), perchlorate (ClO_4^-) [14], selenite (SeO_4^{2-}) [14], chromate ($Cr_2O_4^{2-}$) [2], and bromate (BrO_3^-) [14], as well as organics such as trichloroethylene (C_2HCl_3) [15] and chloroform ($CHCl_3$) [15]. The biofilm on a membrane is responsible for the biodegradation of water contaminants in innocuous products, such as N_2, Cl^-, Se^0, $Cr(OH)_3$, Br^-, ethane, and/or CH_4. In particular, H_2-based MBfRs have been found to be promising for removing NO_3^- from ground and drinking water. For instance, by employing a continuously stirred H_2-based MBfR, a nearly complete removal of NO_3^- from a 40 mg NO_3^--N/L-influent can be achieved [16]. MBfRs have also been reported to remove soluble heavy metal effectively. The rapid reduction of 1000 μg/L Cr(VI) to Cr(III) under denitrifying conditions was carried out in the H_2-based MBfR [2]. In recent years, a CH_4/O_2-based MBfR has drawn attention [17]. Compared to H_2, CH_4 is commonly generated by wastewater treatment plants and landfills [18], and thus can be acquired conveniently and economically. Moreover, the greenhouse effects of CH_4 can be significantly reduced by the stabilization of a CH_4/O_2-based MBfR. Thus far, no reports or studies have investigated the application of a CH_4/O_2-based MBfR to simultaneously treat NO_3^- and Cr.

This study employed a CH_4/O_2-based MBfR for aerobic CH_4 oxidation coupled with denitrification and Cr(VI) reduction. The effects of the partial pressure of intramembrane CH_4 and O_2 on NO_3^- removal, Cr(VI) reduction, and total organic carbon and intermediate products were systematically examined. The functional bacteria and community were also examined using the Next Generation Sequencing technology. Optimal conditions for concomitant Cr(VI) reduction and Cr(III) precipitation in the methane/oxygen-based MBfR were also analyzed and determined.

2. Materials and methods

2.1. MBfR setup

Fig. 1 shows the MBfR schematics used in this study, which had been modified from Xia et al. [19]. The system consisted of a transparent plastic cylinder sealed with a plastic ring, silicone pipelines, and peristaltic pumps (Lange BT100-2J, China). The reactor was 30 cm in height and 12 cm in inner diameter. All of the membranes used in the reactor were polyvinylidene fluoride (PVDF) hollow fibers with an outer diameter of 0.18 cm, an inner diameter of 0.12 cm, and an average pore size of 0.01 μm (Litree Company, Suzhou, China). The reactor contained two main bundles (100 fibers each) that were 30 cm long. Both ends of the main bundles were connected to the CH_4 gas-delivering pipelines. There were also 25-cm supplementary bundles (65 fibers) pressurized with pure O_2. The total surface areas of the CH_4 and O_2-delivering membranes were 3391.2 and 918.45 cm^2, respectively.

2.2. Enrichment of aerobic methane-oxidizing and denitrifying organisms

The initial activated sludge was collected from an anoxic tank in the Quyang wastewater treatment plant (Yangpu, Shanghai). The domestication media contained the following elements (mg/L): $CaCl_2{\cdot}2H_2O$, 1; $MgCl_2$ 10; $FeSO_4{\cdot}7H_2O$ 1; $ZnSO_4{\cdot}7H_2O$ 0.013; H_3BO_3 0.038; $CuCl_2{\cdot}2H_2O$ 0.001; $Na_2MoO_4{\cdot}2H_2O$ 0.004; $MnCl_2{\cdot}4H_2O$ 0.004; $CoCl_2{\cdot}6H_2O$ 0.025; $NiCl_2{\cdot}6H_2O$ 0.001; and Na_2SeO_3 0.003. 2 mM Phosphates were added into the feed water to stabilize the pH at 7.2 ± 0.5 throughout the process. Cultivation of the organisms was carried out in 250 ml physiologic salt water bottle with excessive CH_4 and O_2 (1:1 in mole ratio) as the sole electron donor and carbon source, respectively, and 30 mg/L NO_3^- as the sole electron acceptor and nitrogen source. Physiologic salt water bottles were put in the shaking table with 180 rpm and 30 °C. After 2 days as NO_3^- in the bottle decreased below detect limit, a highly enriched aerobic methane-oxidizing and denitrifying culture originating from activated sludge was used as the inoculum.

2.3. Synthetic media preparation and MBfR operation

The composition of synthetic wastewater was (mg/L): $CaCl_2{\cdot}2H_2O$, 1; $MgCl_2$ 10; $FeSO_4{\cdot}7H_2O$ 1; $ZnSO_4{\cdot}7H_2O$ 0.013; H_3BO_3 0.038; $CuCl_2{\cdot}2H_2O$ 0.001; $Na_2MoO_4{\cdot}2H_2O$ 0.004; $MnCl_2{\cdot}4H_2O$ 0.004; $CoCl_2{\cdot}6H_2O$ 0.025; $NiCl_2{\cdot}6H_2O$ 0.001; and Na_2SeO_3 0.003. 2 mM Phosphates were added into the feed water to stabilize the pH at 7.2 ± 0.5 throughout the process. The DO level in the influent was 8.3 ± 0.2 mg/L.

As shown in Table 1, the operation was divided into four stages. In stage 1, 150 mL suspended biomass of the previous enriched aerobic methane-oxidizing and denitrifying culture was injected into the reactor using a sterilized syringe. The CH_4 supply pressure was set at 0.02 MPa, however, O_2 was not provided. After DO in a reactor decreased below 1.0 ppm [10], the CH_4 pressure was increased to 0.05 MPa and the O_2 pressure was adjusted to 0.03 MPa to maintain the DO concentration around 0.4–1.0 mg/L for biofilm accumulation. In stage 2, Cr(VI) (dichromate) was first

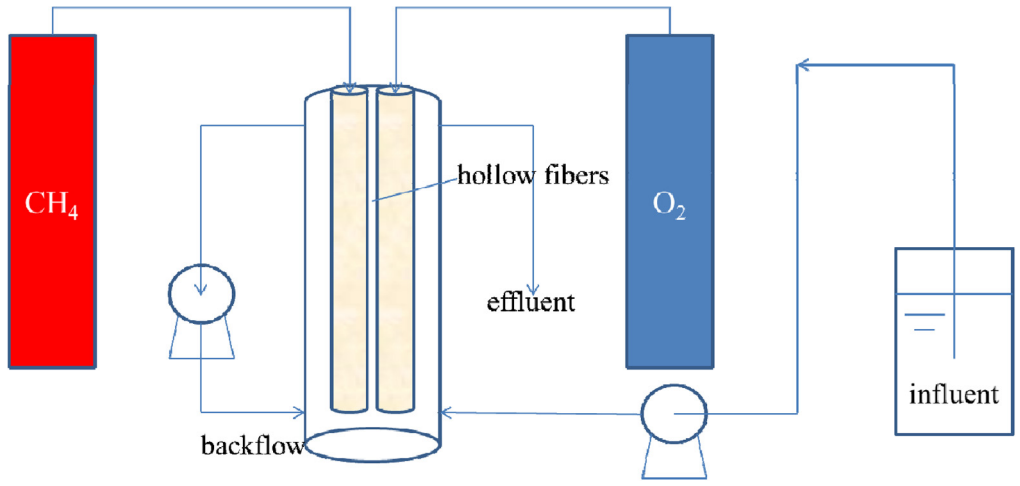

Fig. 1. A schematic of the bench-scale reactor used in the study.

Table 1
Start-up and steady state of the MBfR.

Stages	Influent NO_3^--N concentration (mg/L)	Influent Cr(VI) concentration (μg/L)	CH_4 pressure (MPa)	O_2 pressure (MPa)	Duration (d)
1	10	0	0.02	0	15
2	10	100	0.05	0.03	5
3	20	1000	0.05	0.03	5
4	20	2000	0.05	0.03	19

added to the influent with 100 μg Cr/L and then gradually increased to 1000 μg Cr/L. In stage 3, 1000 μg Cr/L of Cr and 20 mg N/L of NO_3^- were placed simultaneously into the reactor. In stage 4, the concentration of Cr(VI) was increased to 2000 μg Cr/L. All experiments (HRT = 48 h) were conducted at ambient temperature (25 ± 1 °C) and controlled by air conditioning.

2.4. Sampling and analysis

Influent and effluent liquid samples (25 mL) were collected and filtered through a 0.45-μm polyether sulfone syringe filter (Anpel Company, Shanghai, China). Approximately 10 mL samples were also collected without filtration and stored at 4 °C for the total (Cr) measurement using inductively coupled plasma-optical emission spectrometry (ICP-OES) (Agilent 720ES, USA). The Cr(VI) concentration was analyzed by a diphenyl carbazide method (DPC Method, GB7467-87). DPC method was as follow: A 0.4 ml sample of DPC solution (0.2 g DPC dissolved in 50 ml acetone, and then diluted to 100 ml) was added to 10 ml test-tube and the solutions were mixed on a vortex mixer. This was followed by the addition of 0.1 ml H_2SO_4 (50 ml H_2SO_4 (ρ = 1.84 g/ml) dissolved in 50 ml water) and 0.1 ml H_3PO_3 (50 ml H_3PO_3 (ρ = 1.69 g/ml) dissolved in 50 ml water) with further mixing. The magenta color was subsequently compared with standard Cr(VI) solutions at 540 nm after 20 min. All analyses were conducted in triplicate. The Cr(III) concentration was determined by subtracting Cr(VI) from the total (Cr) concentration. Nitrate was determined by an ultraviolet spectrophotometer (HACH, USA) at a wavelength of 220/275 nm following the standard method that eliminated the potential influence of Cr species on the nitrate measurement accuracy. The pH and DO concentrations were measured using a HQ40d meter (HACH, USA). Dissolved organic carbon (DOC) was measured using a total organic carbon analyzer (Shimadzu TOC-5000A, Japan). The intermediate products of CH_4 oxidation were detected with GC-FID (Agilent GC6890N, USA). Hollow fibers were cut off as biofilm samples and the remaining fibers were sealed.

2.5. Flux analysis

The substrate flux of the biofilm on the membrane (J) was calculated to indicate the removal performance of the bioreactors under various conditions, as shown in Eq. (1) [6]:

$$J = \frac{Q(S_i - S_e)}{A}, \quad (1)$$

where J refers to the flux, $g/m^2/d$; Q refers to the influent flow rate, m^3/d; S_i and S_e refer to the influent concentration and the effluent concentration of the substrate (Cr and NO_3^-), respectively, g/m^3; and A refers to the effective surface area of the membrane, m^2.

2.6. Microbial community analysis

Forty-eight days after the MBfR reached a steady state as indicated by stable influent or effluent concentrations of Cr and NO_3^-, the biofilm samples were taken from the bioreactor using a scissor kit for DNA extraction. NGS library preparations and Illumina MiSeq sequencing were conducted at GENEWIZ, Inc. (Beijing, China). DNA samples were quantified using a Qubit 2.0 Fluorometer (Invitrogen, Carlsbad, CA, USA) and DNA quality was checked in a 0.8% agarose gel. About 5–50 ng of the DNA sample was used to generate amplicons using a MetaVx™ Library Preparation kit (GENEWIZ, Inc., South Plainfield, NJ, USA). A panel of proprietary primers was designed to anneal to the relatively conserved regions bordering the V3, V4, and V5 hypervariable regions. The V3 and V4 regions were amplified using forward primers containing the sequence "CCTACGGRRBGCASCAGKVRVGAAT" and reverse primers containing the sequence "GGACTACNVGGGTWTCTAATCC". The V4 and V5 regions were also amplified using forward and reverse primers containing the sequence "GTGYCAGCMGCCGCGGTAA" and "CTTGTGCGGKCCCCCGYCAATTC", respectively. In addition to the 16S rRNA genes target-specific sequence, the primers also contained adaptor sequences that allowed for uniform amplification

of the library with high complexity ready for downstream NGS using Illumina Miseq.

DNA libraries were validated using an Agilent 2100 Bioanalyzer (Agilent Technologies, Palo Alto, CA, USA). DNA libraries were multiplexed and loaded on an Illumina MiSeq instrument according to the manufacturer's instructions (Illumina, San Diego, CA, USA). Sequencing was performed using a 2×250 or 2×300 paired-end (PE) configuration. An image analysis and base calling were conducted using MiSeq Control Software (MCS) on the MiSeq instrument. The sequences were processed and analyzed by GENEWIZ. An taxonomy analysis was carried out on the QIIME platform [20].

2.7. Characterization of biofilm

Fiber membrane samples were taken after 30 days of Cr(VI) addition to characterize the biofilm growth on the outer membrane surface. The preparation of membrane samples for electron microscopy (SEM) image scanning and an energy dispersive X-ray (EDX) followed the procedure as modified from Sutton et al. [21]. A piece of 5-cm hollow-fiber membrane was immersed in 2.5% (V/V) glutaraldehyde solution for 4 h and then rinsed with 16-mM phosphate buffer at pH 7.1. The sample was dehydrated using increasing concentrations of ethanol (once in 10%, 30%, 50%, 70%, and 90%; twice in 100%) for 15 min each. Finally, the samples were frozen at −20 and −70 °C for 12 h each time. The SEM-EDX analyses were then completed using an Ultra High resolution hot field-emission scanning electron microscope (Merlin Compact, Zeiss) according to the manufacturer's instructions (OXFORD_X-MAX, England) at an electron-accelerating voltage of 20.0 kV for elemental composition of the insoluble precipitates in Cr-reducing biofilms.

To analyze Cr(VI) on the fiber membrane samples, about one gram of dried samples was accurately weighed and digested with 10 mL of 50% HNO_3 solution and left overnight. The final extracts were filtered into 25-mL flasks and then diluted to a 1% HNO_3 solution. Finally, Cr(VI) were determined by an ultraviolet spectrophotometer at a 540-nm wavelength.

To characterize the Cr element in the biofilm samples by X-ray diffraction (XRD), the collected samples were first washed with phosphate-buffered saline (PBS, pH = 7.1) for 30 min and then freeze dried by lyophilizer for 48 h, and ground to powder. The analysis of the sample was carried out with a Rigaku Diffractometer (Bruker D8 advance XRD, Germany) using CuKα radiation between 10 and 90° (2θ).

Before and after the addition of NO_3^- and Cr(VI), the biofilm were lyophilized and analyzed for the functional groups using a Fourier-transform infrared (FTIR) spectrometer Nicolet 5700 at room temperature. The spectra were recorded in the wavenumber range of 4000–400 cm^{-1} at a resolution of 5 cm^{-1} with 16 scans.

2.8. Optimal conditions for concomitant Cr(VI) reduction and Cr(III) precipitation

After operating the MBfR for about 48 days, the reactor was operated under different NO_3^- loadings, CH_4/O_2 pressures, and Cr loadings (Table 2). Prior to switching to the next stage, the reactor was operated for 2 days under the "default" condition with 20 mg N/L of NO_3^-, 0.05 MPa of CH_4 and O_2 pressure and 2000 μg /L of Cr. For each short-term stage, conditions were run for three days before effluent samples were collected. With a hydraulic retention time (HRT) of 24 h in the MBfR, 3 days (i.e. 3 HRTs) was sufficient for the system to reach a pseudo-steady state [2], which was defined as pollution concentrations reaching a stable state as well as the biofilm accumulation and biomass not changing significantly. In stage A1–A4 (Table 2), the influent concentration of NO_3^--N varied from 10 to 60 mg N/L, while the CH_4/O_2 pressures and Cr(VI) concentration were fixed at 0.05 MPa and 2000 μg Cr/L, respectively. In stages B1–B4, the system operated at different influent concentrations of Cr(VI) from 300 to 2000 μg Cr/L under the fixed NO_3^- concentration and CH_4/O_2 pressure of 20 mg N/L and 0.05 MPa, respectively. In stages C1–C4, CH_4/O_2 pressure was varied from 0.02 to 0.06 MPa, while the NO_3^- and Cr(VI) concentrations were fixed at 20 mg N/L and 2000 μg Cr/L, respectively. When each stage reached a pseudo-steady state, three effluent samples were collected on the fourth, fifth, and sixth days after the three consecutive days of operation for analyzing different parameters. The final results were shown as the average value and standard deviation of triplicate measurements.

2.9. Statistical analysis

All data were presented from the mean of three measurements ± standard error. The standard error and significance level were calculated using SPSS version 20.0 software. One-way analysis of variance (ANOVA) with a Tukey *post hoc* test was performed to calculate the statistical significance between the mean values. Differences were considered significant if $p < 0.05$.

3. Results and discussion

3.1. Start up and non-steady-state test

Fig. 2 shows the concentrations and removal efficiencies of Cr (VI), Cr(III), total (Cr) and NO_3-$^-$N at the four stages of the 48-day MBfR operation. In stage 1, the 10 mg/L NO_3^- was added into the MBfR as the sole electron acceptor with 0.02 MPa CH_4 present only for 17 days. During the initial three-day batch-mode operation, the NO_3^- removal efficiency was greater than 92%. The biofilms were observed to be immobilized on the fiber surfaces (supplementary data Fig. S1). As the continuous feeding mode with an HRT of 48 h began, the NO_3^- removal slightly decreased and finally stabilized at 76.9 ± 5.2% from day 10 to day 17.

In stage 2, over the next five days, 100 μg/L Cr(VI) along with 0.05 MPa O_2 were introduced into the MBfR. Cr(VI) was rapidly removed by 90.1% within one day while the NO_3^- removal remained at 76.0 ± 3.9%.

During the next two stages, the NO_3^- concentration was doubled to 20 mg N/L, and the Cr(VI) concentration was adjusted to 1000 and 2000 μg Cr/L in stages 3 and 4, respectively. Despite the greatly increased Cr(VI) loading, its reduction rate was still high (98.9% for stage 3 and 98.7% for stage 4) without a significance difference ($p = 1.000$). The Cr(VI) was reduced to Cr(III), and then Cr(III) precipitates were deposited on the biofilm, which was verified by SEM/EDX. At stages 3 and 4, the NO_3^- removal efficiency was also ⩾95%. This demonstrated that Cr(VI) at the applied level did not inhibit NO_3^--reducing microorganisms in the MBfR system. The effluent Cr(VI) level remained low and stable (~25 μg/L) even when the influent Cr(VI) was increased by 10-fold (2000 μg/L), indicating that the Cr(VI)-removal capacity of the biofilm increased throughout the test period.

Fig. 3 shows the changes of DO, pH, and VFAs in the bioreactor during the four stages as separated by the dotted lines. The DO varied from 0.1 to 1.0 mg/L, while the pH also fluctuated between 6 and 7.5 with a slight trend of decline after stage 3. The effluent pH, in the range of 6.5 to 7.5, was slightly lower than the influent pH (7.5). Fig. 3a shows the compositional changes of the VFAs in the four stages. The total amount of VFAs declined over time from 5 ppm to less than 3 ppm. Acetate was the main product (>30% in all stages) among the accumulated VFAs, which may explain

Table 2
Short-time reactor experiments.

Stages	Influent NO_3^--N concentration (mg/L)	Influent Cr(VI) concentration (mg/L)	CH_4 and O_2 pressure (Mpa)	Duration (day)	Influent pH	Influent DO (ppm)
A1	10	2	0.05	8	6.40	0.57
A2	20			8	6.85	0.53
A3	40			8	6.44	0.30
A4	60			8	6.60	0.31
B1	20	2	0.02	8	6.57	0.91
B2			0.03	8	6.44	0.95
B3			0.05	8	6.49	0.42
B4			0.06	8	6.76	0.38
C1	20	0.3	0.05	8	6.57	0.91
C2		0.05		8	6.44	0.95
C3		1		8	6.49	0.42
C4		2		8	6.76	0.38

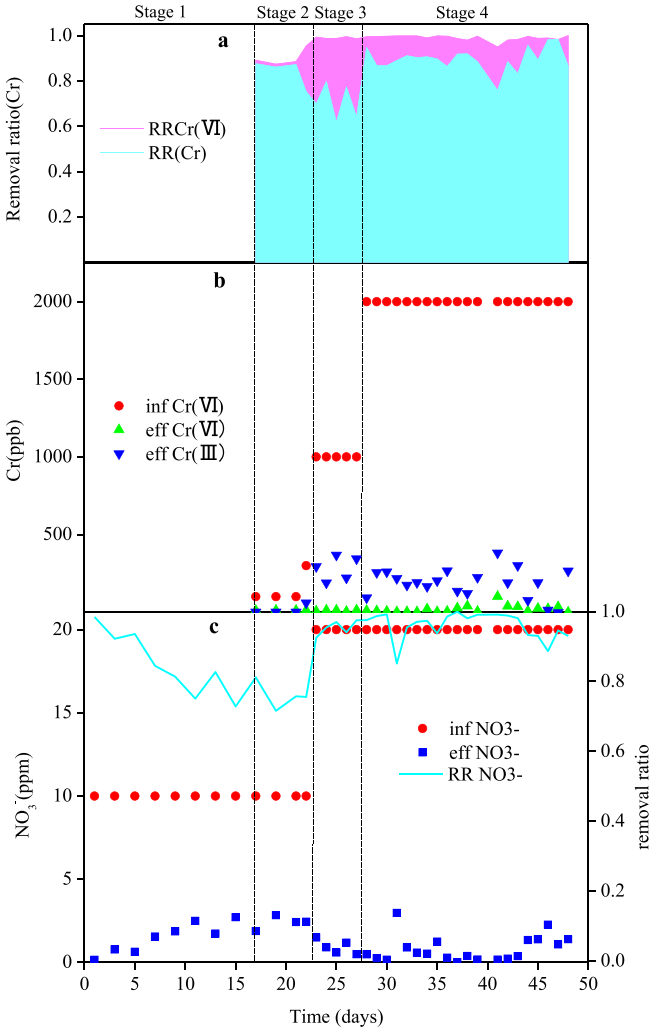

Fig. 2. (a) The total (Cr), Cr(VI) removal rate (RR); (b) concentrations of influent Cr (VI) (ppb), effluent Cr(VI) (ppb), and effluent Cr(III) (ppb); and (c) concentrations of influent NO_3^--N (ppm), effluent NO_3^--N (ppm), and NO_3^--N removal ratio in the MBfR.

the decrease of pH. The products of methane and oxygen by methanotrophs is speculated to be methanol [22] and methanol-utilizing denitrifiers are believed to coexist with methanotrophs, consuming the produced organic substances by methanotrophs as alternative electron donors [23]. Acetate and proteins [23] have also been suggested as intermediate products.

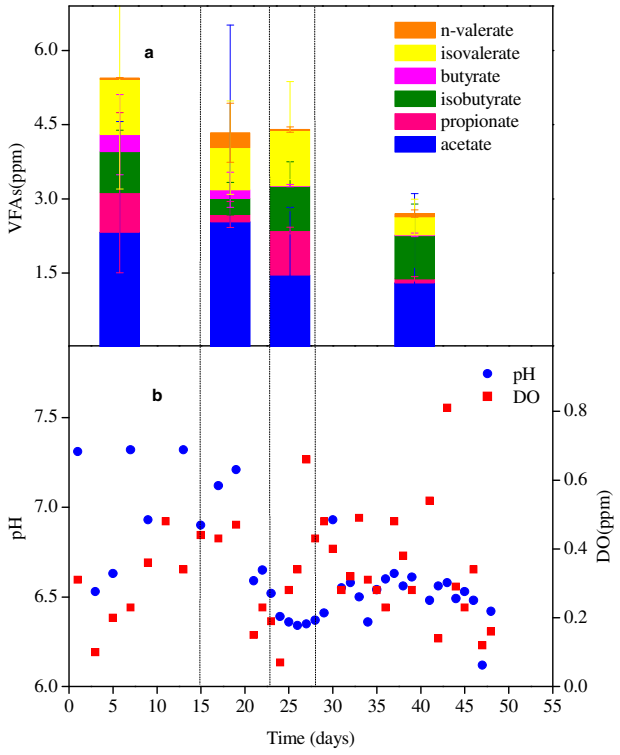

Fig. 3. (a) Average concentrations of VFA products in the four stages (ppm); (b) pH and DO in the MBfR during the four stages (ppm).

In our study, methanol was not detected because it was easily utilized by microorganisms [10]. VFAs were detected as the products of methane and oxygen. Bacteria capable of denitrification on all those organics were found; however, the volume required for acetate or protein was smaller compared to the volume required for methanol, indicating the less accumulation of methanol [10]. Our Dissolved Organic Carbon (DOC) tests (supplementary data Fig. S2) shows that the effluent DOC concentration is higher than the DOC of VFAs, which may be attributed to the generation of soluble microbial products (SMP) during the growth of microorganisms [24]. In addition, methanotrophs have been shown to release nucleic acids and carbohydrates as lysis products or soluble metabolites under certain environmental conditions [10]. Most likely a mixture of organics produced by the methanotrophs are utilized by the denitrifiers [10].

O_2 is the most important factor in aerobic methane oxidation coupled to denitrification [10]. This process can be carried out by a microbial consortium consisting of aerobic methanotrophs

oxidizing methane and facultatively anaerobic denitrifiers using organic compounds released by the methanotrophs as the electron donor. The first oxidation of methane to methanol is catalyzed by methane monooxygenase (MMO). However, the presence of DO can suppress the enzyme system needed for denitrification. So it should be noted that the DO always remains below 1.0 mg/L [22]. So in this process, DO is controlled below 1.0 mg/L. And the accumulation of organics indicates that DO below 1.0 mg/L is appropriate for methanotrophs. Simultaneously, the effect of denitrification shows that it is fit for denitrifiers.

3.2. Microbial community analysis

Fig. 4 showed that the microbial community between the initial inoculated sludge and enriched biomass in the methane/oxygen-based MBfR operation had obvious shifts. The phylogenetic classification in Fig. 4a showed that all of the sequences were grouped in bacterial phyla. In the reactor, *Proteobacteria* (66%) and *Bacteroidetes* (24%) were the most dominant phyla, which collectively comprised ~90% of the total sequences. Many types of denitrifiers are included in the phyla of *Proteobacteria* and *Bacteroidetes* [25].

Fig. 4b showed that the addition of Cr(VI) enhanced the growth of the Cr(VI) reducers. For example, the family *Comamonadaceae* was enriched from 4.36% in the anoxic sludge to 6.78% of the whole community in the bioreactor. Meanwhile, methane as the carbon source noticeably shifted the community at a family level, and consequently, methanotrophic bacteria dominated the CH_4/O_2-based MBfR. In the biofilm, the majority of sequences belonged to the family *Methylococcaceae* (18.7% of the whole community in the reactor compared with 0.03% in the anoxic sludge), with sequences clustering into the genus *Methylococcus* in MBfR biofilms (supplementary data Fig. S3). *Methylococcus* is a kind of methanotroph that can convert methane and oxygen into methanol [26]. The family *Methylophilaceae* was another methanotrophic bacteria [27] that was enriched in the biofilm. *Chitinophagaceae*, a group of heterotrophic bacteria capable of hydrolyzing some organic matter [28], were three times enriched (14.7% in MBfR) compared to the level in anoxic sludge, which was due to the accumulated organics. In comparison to the enriched Cr(VI) reducer and methanotrophs, the dominant denitrificans at family level shifted from *Rhodocyclaceae* [29] and *Xanthomonadaceae* [30] (11.6% in anoxic sludge) to *Cytophagaceae* [31], *Hyphomicrobiaceae* [32], *Comamonadaceae* [29] and *Alcaligenaceae* [33] (18.9% in the reactor). In particular, *Comamonadaceae* could reduce nitrate and Cr(VI) simultaneously and could be responsible for the enhanced removal of nitrate and Cr(VI).

3.3. The fate of Cr

Effluent samples from MBfR were assayed by ICP each for the total Cr concentration with and without filtration. However, the results were not significantly different. The possible reason was that most of Cr(VI) was reduced to Cr(III), and then precipitated in the form of hydroxides and adsorbed on the biofilm [34]. To examine this hypothesis, biofilm samples were collected and analyzed using ICP, SEM-EDX, XRD, and FTIR.

The DPC results showed that Cr(VI) was below the detectable limit, which indicated that little Cr(VI) existed in the biofilms. Fig. 5a and b showed the surface morphology of the hollow fiber and the biofilm growing attached to the fiber surface from the Cr-reducing MBfR. The fiber PVDF membrane had a microporous structure, and the biofilm had a thickness of about 33 μm with rod- and coccus-shaped bacteria observed. The EDS analysis in Fig. 5d showed a noticeable Cr peak compared with the pristine

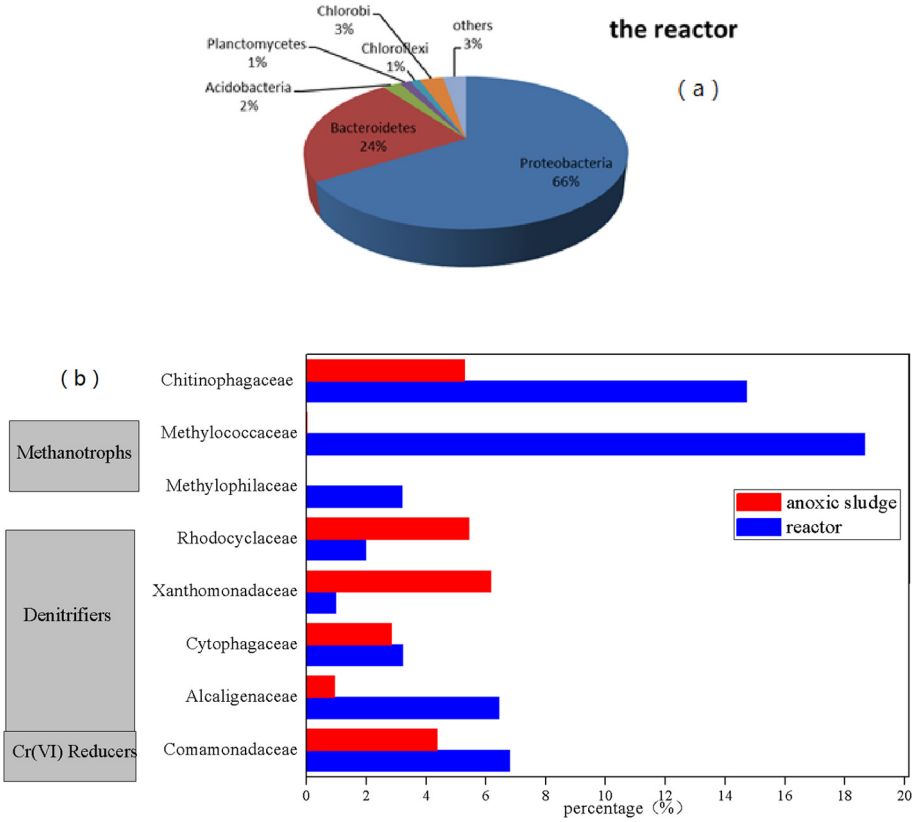

Fig. 4. Relative abundance of bacterial community composition in two samples (the reactor and anoxic sludge): (a) the relative abundance of total bacteria grouped by phylum, (b) the relative abundance of the total bacteria grouped by family

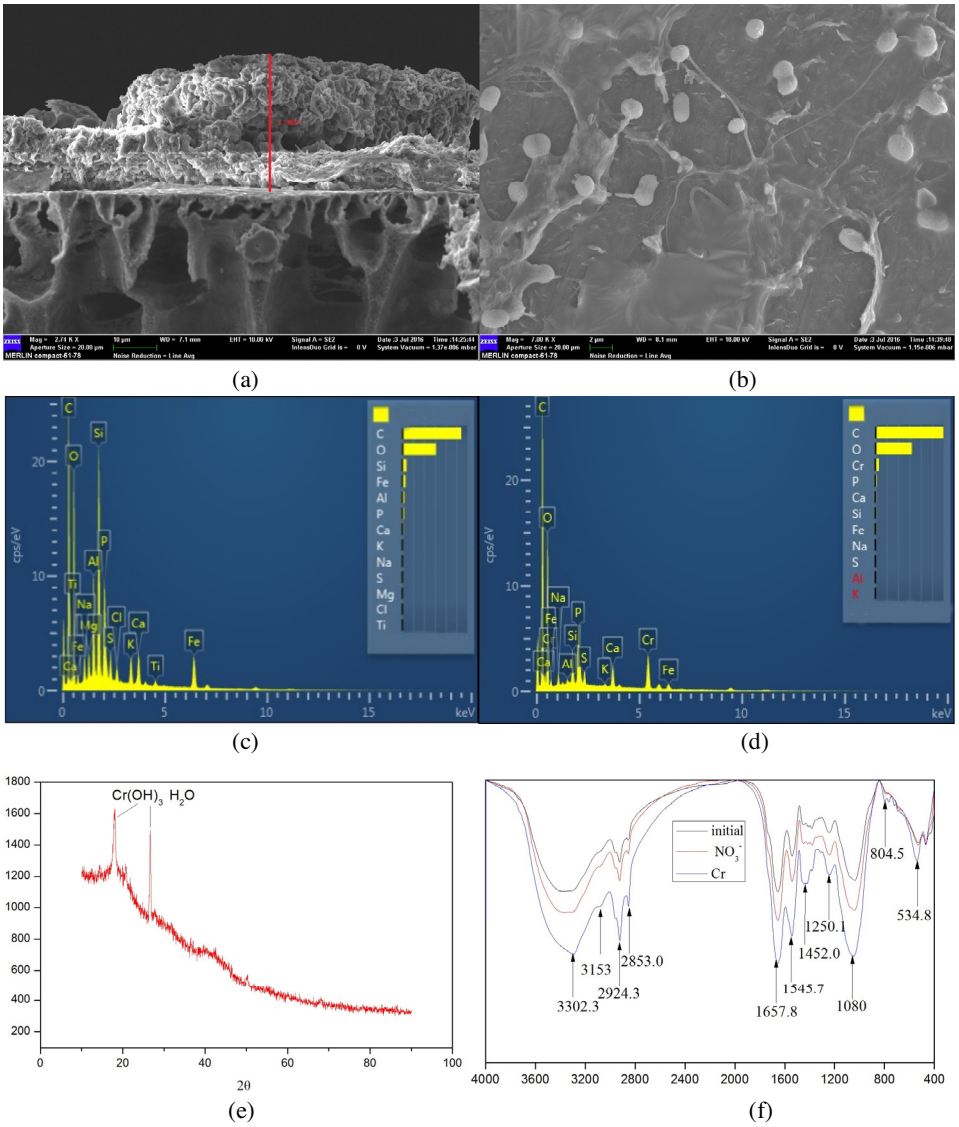

Fig. 5. (a) Scanning electron micrograph of section fiber; (b) surface biofilm from MBfR; (c) an EDX of the initial biofilm; (d) an EDS obtained from the insoluble precipitate formed in Cr(V)-reducing biofilm and the random area from reactor; (e) an XRD analysis of biofilm; (f) an FTIR analysis of the biofilm before and after the addition of NO_3^- and Cr.

PVDF membrane in Fig. 5c, which demonstrated that Cr was adsorbed onto the biofilm. The XRD patterns for biofilms in Fig. 5e. indicated that chromic hydroxide [$Cr(OH)_3{\cdot}H_2O$] existed on the biofilm at 2θ of 18.08° and 26.7°, which was indicative of the deposition of Cr(III) precipitate on the biofilm. This was probably because that the effluent pH was in the range of 6.5–7.5. In this range, The reduced effluent Cr(III) concentration in our system was ~200 μg/L, which was close to the conditional solubility of Cr(III) for pH 6.5–7.5 (i.e., 50–200 μg/L) [2]. Thus, most of Cr(III) became precipitate in the forms of chromic hydroxide [$Cr(OH)_3{\cdot}H_2O$].

The FTIR results in Fig. 5f further indicate the adsorption of Cr (III) on the biofilm. The FTIR spectra of the biofilm before (initial and NO_3^--reduction biofilm) and after Cr adsorption are compared in Fig. 5f. The FTIR of nitrate reduction biofilm is similar to the initial biofilm, while the addition of Cr shifts the adsorption peaks a lot. The shifts in the adsorption peaks showed the possible involvement of the hydroxyl, nitro, carboxyl, and sulfonate groups of the biofilm fraction in Cr binding [35]. The biofilm samples displayed a broad, stretching, intense peak at around 3302 cm^{-1}, which was characteristic of the stretching of —OH [36]. The adsorption band of the two samples at 2924 cm^{-1} was characteristic for the stretching vibration of —CH [36]. The adsorption peak at 1658 cm^{-1} and 1452 cm^{-1} indicated the stretching vibration of C═C and asymmetric stretching vibration of C—O—C, which were involved in the sorption process due to the palpable deviation [35,36]. A new adsorption band at around 3153 cm^{-1} appeared after the deposition of Cr on the biofilm. Apparently, two new peaks were formed at 805 cm^{-1} and 535 cm^{-1}, which were also called the "fingerprint" zone, and were characteristic of phosphate or sulfur functional groups [37].

3.4. Optimization of concomitant Cr(VI) reduction and Cr(III) precipitation

3.4.1. The influence of NO_3^--N on Cr(VI) reduction and Cr(III) precipitation

Previous research has found that NO_3^--N is a priority electron acceptor in H_2-based MBfRs [6]. Thus, although a high NO_3^- loading may inhibit the reduction of Cr(VI), in a methane/oxygen-based MBfR, the competitive relation has changed.

As shown in Fig. 6a, the effluent Cr(VI) and NO_3^- concentrations modestly increased when the influent NO_3^- concentration increased from 10 mg N/L to 40 mg N/L. When the inflow NO_3^--N was 60 mg/L, the concentration of Cr(VI) in the effluent rose to 348.5 ± 61.0 μg Cr/L with a decrease in the removal rate for Cr (VI), which was consistent with previous research that heterotrophic denitrification and Cr(VI) reduction took place simultaneously [38]. However, NO_2^-, the intermediate products of NO_3^- reduction, may inhibit Cr(VI) reduction [39,40]. At the same time, Cr(VI) would also inhibit NO_2^- reduction. Similarly, in H_2-based MBfRs, the increasing concentration of NO_3^- was reported to inhibit the removal of Cr(VI) due to the consumption of H_2 and electrons [2]. In our case, high NO_3^- resulted in the consumption of CH_4 and production of CO_2 that promoted Cr(III) precipitation [10]:

$$3CH_4 + 3O_2 + \frac{12}{5}NO_3^- + \frac{12}{5}H^+ = \frac{6}{5}N_2 + \frac{36}{5}H_2O + 3CO_2. \quad (2)$$

3.4.2. Organic electron donor source for Cr(VI) reduction

In previous studies of H_2-based MBfRs, H_2 partial pressure was recognized as a key parameter [2,6]. Similarly, in the CH_4/O_2-based MBfR, the CH_4 partial pressure is also important for the Cr(VI) conversion. As shown in Fig. 6b, the NO_3^- reduction was significantly enhanced as the CH_4 pressure increased. However, the effluent Cr (III) concentration was stable (134 μg Cr/L) at different CH_4 partial pressures. Increasing CH_4 pressure also caused a steady decrease in effluent Cr(VI), and the total(Cr), which reached 1989.0 ± 2.9 μg Cr/L and 1887.3 ± 48.3 μg Cr/L at 0.06 MPa, respectively. The increase of CH_4 partial pressure may have increased the biofilm activity and promoted the generation of organic substrate (e.g., VFAs) as an electron donor for NO_3^- and Cr(VI) reduction. However, further increasing the applied CH_4 pressure from 0.05 MPa to 0.06 MPa did not appreciably increase the Cr and NO_3^- reduction, which suggested that the partial pressure of CH_4 higher than 0.05 MPa may not be a limiting factor in the present system.

3.4.3. Optimal Cr(VI) loading

The effluent concentration of NO_3^- was not significantly affected as the influent Cr(VI) increased (Fig. 6c). The effluent Cr(VI) concentration also remained at a low level, even with an increase of influent Cr(VI) concentration from 300 to 2000 μg Cr/L. The removal fluxes and removal efficiencies of Cr(VI) were 4.91 and 33.9 mg/m^2/d, and 99.8% and 96.3%, respectively, indicating that the CH_4/O_2-based MBfR has a high resiliency for Cr(VI) loading. This resiliency could be attributed to high adaptability of the Cr (VI) reducers in the biofilm [2].

As the Cr(VI) loading increased, so did the effluent Cr(III) concentration. This was because at a high-influent Cr(VI) (1000 and 2000 μg Cr/L), the CO_2 alkalinity generation from Eq. (2) could be inhibited due to competition with NO_3^- on the available CH_4. Therefore, the alkalinity may not be sufficient for Cr(III) to precipitate. Clearly, NO_3^-, CH_4 partial pressure, and Cr(VI) concentration should be set properly in order to remove Cr more efficiently. The condition of 0.05 MPa, 2000 μg Cr/L, and 40 mg N/L may be suitable for the optimal Cr(VI) reduction and Cr(III) precipitation.

In the CH_4/O_2-based MBfR, *Methylophilaceae* and *Methylococcaceae* utilize methane and oxygen to produce methanol and VFAs, which are supplied as electron donor for coexisting denitrifiers and Cr(VI) reducers. Denitrifying bacteria reduce nitrate to nitrogen, while Cr(VI) is reduced to Cr(III) and then precipitated at proper alkalinity and adsorbed onto the biofilm.

4. Conclusion

This study demonstrated the synergies of a CH_4/O_2-based MBfR for the removal of NO_3^- and Cr(VI) via reduction and precipitation. Acetate was a main product of CH_4 oxidation. According to the

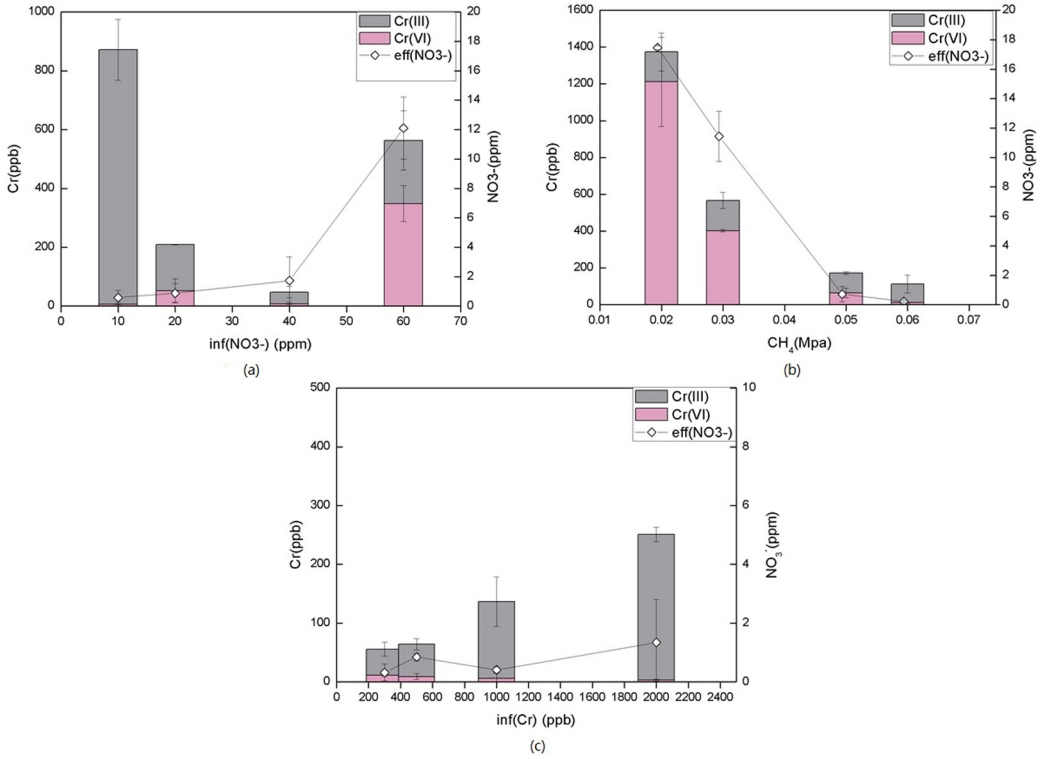

Fig.6. The average concentrations of effluent NO_3^- and Cr(VI)/Cr(III) at steady states of the short-term stages for (a) varied nitrate loadings; (b) varied CH_4 partial pressures; and (c) varied Cr(VI) loadings.

results of the next generation sequence, denitrifiers (e.g., *Comamonadaceae*, *Cytophagaceae*, *Hyphomicrobiaceae*, *Alcaligenaceae*), methanotrophs (e.g., *Methylophilaceae* and *Methylococcaceae*) and chromium reducing organisms (e.g., *Comamonadaceae*) were detected in the microbial community. It was demonstrated through ICP, SEM-EDX, XRD and FTIR analyses that most of the reduced Cr remained in the form of precipitates and adsorbed onto the biofilm. Short-term experiments confirmed that influent NO_3^-, CH_4 partial pressure, and Cr(VI) significantly affected the rate and extent of Cr(VI) and NO_3^- reduction. These parameters should be set properly to achieve efficient Cr(VI) reduction and Cr(III) precipitation.

Acknowledgements

This work is supported by National Natural Science Foundation of China (No. 51378368 and No. 51678422).

Appendix A. Supplementary data

Supplementary data associated with this article can be found, in the online version, at http://dx.doi.org/10.1016/j.cej.2017.01.018.

References

[1] J. Barnhart, Occurrences, uses, and properties of chromium, Regul. Toxicol. Pharm. 26 (1997) S3–S7.
[2] J. Chung, R. Nerenberg, B.E. Rittmann, Bio-reduction of soluble chromate using a hydrogen-based membrane biofilm reactor, Water Res. 40 (2006) 1634–1642.
[3] T.L. Rinehart, D.G. Schulze, R.M. Bricka, S. Bajt, E.R. Blatchley, Chromium leaching vs. oxidation state for a contaminated solidified/stabilized soil, J. Hazard. Mater. 52 (1997) 213–221.
[4] US EPA, National Primary Drinking Water Standard. EPA 816-F-03-016, Office of Groundwater and Drinking Water (4606 M), Washington, D.C., 2003.
[5] S. Xia, X. Xu, C. Zhou, C. Wang, L. Zhou, B.E. Rittmann, Direct delivery of CO2 into a hydrogen-based membrane biofilm reactor and model development, Chem. Eng. J. 290 (2016) 154–160.
[6] S. Xia, J. Liang, X. Xu, S. Shen, Simultaneous removal of selected oxidized contaminants in groundwater using a continuously stirred hydrogen-based membrane biofilm reactor, J. Environ. Sci. 25 (2013) 96–104.
[7] L. Peng, Y. Liu, S.-H. Gao, X. Chen, B.-J. Ni, Evaluating simultaneous chromate and nitrate reduction during microbial denitrification processes, Water Res. 89 (2016) 1–8.
[8] P. Gikas, P. Romanos, Effects of tri-valent (Cr(III)) and hexa-valent (Cr(VI)) chromium on the growth of activated sludge, J. Hazard. Mater. 133 (2006) 212–217.
[9] E. Vaiopoulou, P. Gikas, Effects of chromium on activated sludge and on the performance of wastewater treatment plants: A review, Water Res. 46 (2012) 549–570.
[10] O. Modin, K. Fukushi, K. Yamamoto, Denitrification with methane as external carbon source, Water Res. 41 (2007) 2726–2738.
[11] O. Modin, K. Fukushi, F. Nakajima, K. Yamamoto, Aerobic methane oxidation coupled to denitrification: kinetics and effect of oxygen supply, J. Environ. Eng.-ASCE 136 (2010) 211–219.
[12] E. Lie, T. Welander, Influence of dissolved-oxygen and oxidation-reduction potential on the denitrification rate of activated-sludge, Water Sci. Technol. 30 (1994) 91–100.
[13] F. Thalasso, A. Vallecillo, P. GarciaEncina, F. FdzPolanco, The use of methane as a sole carbon source for wastewater denitrification, Water Res. 31 (1997) 55–60.
[14] R. Nerenberg, B.E. Rittmann, Hydrogen-based, hollow-fiber membrane biofilm reactor for reduction of perchlorate and other oxidized contaminants, Water Sci. Technol. 49 (2004) 223–230.
[15] J. Chung, B.E. Rittmann, Simultaneous bio-reduction of trichloroethene, trichloroethane, and chloroform using a hydrogen-based membrane biofilm reactor, Water Sci. Technol. 58 (2008) 495–501.
[16] S. Xia, Y. Zhang, F. Zhong, A continuous stirred hydrogen-based polyvinyl chloride membrane biofilm reactor for the treatment of nitrate contaminated drinking water, Bioresour. Technol. 100 (2009) 6223–6228.
[17] X. Chen, J. Guo, Y. Shi, S. Hu, Z. Yuan, B.-J. Ni, Modeling of simultaneous anaerobic methane and ammonium oxidation in a membrane biofilm reactor, Environ. Sci. Technol. 48 (2014) 9540–9547.
[18] O. Modin, K. Fukushi, F. Nakajima, K. Yamamoto, Nitrate removal and biofilm characteristics in methanotrophic membrane biofilm reactors with various gas supply regimes, Water Res. 44 (2010) 85–96.
[19] S. Xia, C. Wang, X. Xu, Y. Tang, Z. Wang, Z. Gu, Y. Zhou, Bioreduction of nitrate in a hydrogen-based membrane biofilm reactor using CO 2 for pH control and as carbon source, Chem. Eng. J. 276 (2015) 59–64.
[20] J.G. Caporaso, J. Kuczynski, J. Stombaugh, K. Bittinger, F.D. Bushman, E.K. Costello, N. Fierer, A.G. Pena, J.K. Goodrich, J.I. Gordon, G.A. Huttley, S.T. Kelley, D. Knights, J.E. Koenig, R.E. Ley, C.A. Lozupone, D. McDonald, B.D. Muegge, M. Pirrung, J. Reeder, J.R. Sevinsky, P.J. Tumbaugh, W.A. Walters, J. Widmann, T. Yatsunenko, J. Zaneveld, R. Knight, QIIME allows analysis of high-throughput community sequencing data, Nat. Methods 7 (2010) 335–336.
[21] N.A. Sutton, N. Hughes, P.S. Handley, A comparison of conventional SEM techniques, low temperature SEM and the electroscan wet scanning electron microscope to study the structure of a biofilm of Streptococcus crista CR3, J. Appl. Bacteriol. 76 (1994) 448–454.
[22] M. Werner, R. Kayser, Denitrification with biogas as external carbon source, Water Sci. Technol. 23 (1991) 701–708.
[23] A. Eisentraeger, P. Klag, B. Vansbotter, E. Heymann, W. Dott, Denitrification of groundwater with methane as sole hydrogen donor, Water Res. 35 (2001) 2261–2267.
[24] K.C. Lee, B.E. Rittmann, A novel hollow-fibre membrane biofilm reactor for autohydrogenotrophic denitrification of drinking water, Water Sci. Technol. 41 (2000) 219–226.
[25] J. Luo, H. Liang, L. Yan, J. Ma, Y. Yang, G. Li, Microbial community structures in a closed raw water distribution system biofilm as revealed by 454-pyrosequencing analysis and the effect of microbial biofilm communities on raw water quality, Bioresour. Technol. 148 (2013) 189–195.
[26] H. Bothe, K.M. Jensen, A. Mergel, J. Larsen, C. Jørgensen, H. Bothe, L. Jørgensen, Heterotrophic bacteria growing in association with *Methylococcus capsulatus* (Bath) in a single cell protein production process, Appl. Microbiol. Biotechnol. 59 (2002) 33–39.
[27] R. Chen, Y.-H. Luo, J.-X. Chen, Y. Zhang, L.-L. Wen, L.-D. Shi, Y. Tang, B.E. Rittmann, P. Zheng, H.-P. Zhao, Evolution of the microbial community of the biofilm in a methane-based membrane biofilm reactor reducing multiple electron acceptors, Environ. Sci. Pollut. (2016) 1–9.
[28] L. Jin, H.-G. Lee, H.-J. La, S.-R. Ko, C.-Y. Ahn, H.-M. Oh, Ferruginibacter profundus sp. nov., a novel member of the family *Chitinophagaceae*, isolated from freshwater sediment of a reservoir, Anton. Leeuw. 106 (2014) 319–323.
[29] J.H. Park, O. Choi, T.H. Lee, H. Kim, B.I. Sang, Pyrosequencing analysis of microbial communities in hollow fiber-membrane biofilm reactors system for treating high-strength nitrogen wastewater, Chemosphere 163 (2016) 192–201.
[30] G.H. Xu, J.J. Peng, C.J. Feng, F. Fang, S.H. Chen, Y.J. Xu, X.Z. Wang, Evaluation of simultaneous autotrophic and heterotrophic denitrification processes and bacterial community structure analysis, Appl. Microbiol. Biotechnol. 99 (2015) 6527–6536.
[31] M. Golebiewski, E. Deja-Sikora, M. Cichosz, A. Tretyn, B. Wrobel, 16S rDNA Pyrosequencing Analysis of Bacterial Community in Heavy Metals Polluted Soils, Microb. Ecol. 67 (2014) 635–647.
[32] H.Y. Xu, L.P. Chen, S.Z. Fu, H.X. Fan, Y.G. Zhou, S.J. Liu, Z.P. Liu, *Zhangella mobilis* gen. nov., sp nov., a new member of the family Hyphomicrobiaceae isolated from coastal seawater, Int. J. Syst. Evol. Microbiol. 59 (2009) 2297–2301.
[33] S.S. Adav, D.J. Lee, J.Y. Lai, Microbial community of acetate utilizing denitrifiers in aerobic granules, Appl. Microbiol. Biotechnol. 85 (2010) 753–762.
[34] G. Farabegoli, A. Carucci, M. Majone, E. Rolle, Biological treatment of tannery wastewater in the presence of chromium, J. Environ. Manage. 71 (2004) 345–349.
[35] O. Braissant, A.W. Decho, C. Dupraz, C. Glunk, K.M. Przekop, P.T. Visscher, Exopolymeric substances of sulfate-reducing bacteria: Interactions with calcium at alkaline pH and implication for formation of carbonate minerals, Geobiology 5 (2007) 401–411.
[36] M. Iqbal, A. Saeed, S.I. Zafar, FTIR spectrophotometry, kinetics and adsorption isotherms modeling, ion exchange, and EDX analysis for understanding the mechanism of Cd2+ and Pb2+ removal by mango peel waste, J. Hazard. Mater. 164 (2009) 161–171.
[37] G. Guibaud, N. Tixier, A. Bouju, M. Baudu, Relation between extracellular polymers' composition and its ability to complex Cd, Cu and Pb, Chemosphere 52 (2003) 1701–1710.
[38] F. Di Capua, S. Papirio, P.N.L. Lens, G. Esposito, Chemolithotrophic denitrification in biofilm reactors, Chem. Eng. J. 280 (2015) 643–657.
[39] R. Han, J.T. Geller, L. Yang, E.L. Brodie, R. Chakraborty, J.T. Larsen, H.R. Beller, Physiological and transcriptional studies of Cr (VI) reduction under aerobic and denitrifying conditions by an aquifer-derived pseudomonad, Environ. Sci. Technol. 44 (2010) 7491–7497.
[40] P. Chovanec, C.E. Sparacino-Watkins, N. Zhang, P. Basu, J. Stolz, Microbial reduction of chromate in the presence of nitrate by three nitrate respiring organisms, Front. microbiol. 3 (2012) 416.